Helmholtz-Zentrum Dresden-Rossendorf (HZDR)

HZDR
HELMHOLTZ ZENTRUM
DRESDEN ROSSENDORF

Effective Hexagonal Boron Nitride Passivation of Few-Layered InSe and GaSe to Enhance Their Electronic and Optical Properties

Arora, H.; Jung, Y.; Venanzi, T.; Watanabe, K.; Taniguchi, T.; Schneider, H.; Hone, J.; Helm, M.; Erbe, A.; Hübner, R.;

Originally published:

October 2019

ACS Applied Materials and Interfaces 11(2019)46, 43480-43487

DOI: https://doi.org/10.1021/acsami.9b13442

Perma-Link to Publication Repository of HZDR:

https://www.hzdr.de/publications/Publ-29362

Release of the secondary publication
on the basis of the German Copyright Law § 38 Section 4.

Effective hexagonal boron nitride passivation of few-layered InSe and GaSe to enhance their electronic and optical properties

Himani Arora[1,2§], Younghun Jung[3§], Tommaso Venanzi[1,2], Kenji Watanabe[4], Takashi Taniguchi[4], Harald Schneider[1], James C. Hone[3], and Artur Erbe[1*]*

[1] Helmholtz-Zentrum Dresden-Rossendorf, 01328 Dresden, Germany

[2] Technische Universitaet Dresden, 01062 Dresden, Germany

[3] Department of Mechanical Engineering, Columbia University, New York, 10027 NY, USA

[4] National Institute for Materials Science, 1-1 Namiki, 305-0044 Tsukuba, Japan

§ These authors contributed equally

* Correspondence should be addressed to James C. Hone (email: jh2228@columbia.edu) and Artur Erbe (email: a.erbe@hzdr.de)

ABSTRACT:

Recent demonstration of high mobilities in indium selenide (InSe) and, nonlinear optical properties and single-photon emission in gallium selenide (GaSe) has set them as emerging two-

dimensional (2D) semiconductors which can exceed transition metal dichalcogenides in various applications. Yet InSe- and GaSe-based devices are still lagging behind due to their sensitivity to ambience and device fabrication processes which induce structural damage and hamper their intrinsic properties. Thus, in order to achieve high performance and stable devices, effective passivation of these air-sensitive materials is much required. Here we demonstrate a hexagonal boron nitride (hBN) based encapsulation technique, where 2D layers of InSe and GaSe are covered entirely between two layers of hBN. To fabricate devices out of fully encapsulated 2D layers, we employ lithography-free via-contacting scheme. We find that hBN acts as an excellent encapsulant and a near-ideal substrate for InSe and GaSe by passivating them from the ambience and isolating them from the charge disorder at the SiO_2 surface. As a result, the devices fabricated from encapsulated InSe are of high quality, ambient stable and show a greatly improved two-terminal mobility of 30–120 $cm^2V^{-1}s^{-1}$ as compared to mere ~1 $cm^2V^{-1}s^{-1}$ for unencapsulated devices. On employing this technique to GaSe few-layers system, we obtained a strong and reproducible photoresponse with high responsivities up to 84.2 AW^{-1} at 405 nm. This work demonstrates that full hBN encapsulation suppresses the degradation of InSe and GaSe, and maintains high and stable performance of their devices. We believe that this technique can open ways for the fundamental study as well as towards the integration of these materials in technological applications.

KEYWORDS: indium selenide, gallium selenide, hexagonal boron nitride, encapsulation, photoluminescence, stable electronics, field-effect transistors, photodetectors

The III-VI chalcogenide family (MX; M = Ga, In and X = S, Se, Te) has gained immense attention in recent years owing to its interesting properties and underlying physics at low dimensions. Two most prominent members of this family are indium selenide and gallium selenide (InSe and GaSe) which have huge potential in various applications such as high-speed electronics,[1–4] opto-electronics,[5–8] sensors[9–10] and terahertz applications[11]. Recently, InSe-based devices have seen many advancements owing to its high electron mobility[1–3] resulting from its low electron effective mass (m_e^*=0.143 m_o)[12] and a direct band gap lying in the near-infrared (NIR) range[13]. In contrast to transition metal dichalcogenides (TMDCs), where the mobility drops severely on decreasing the layer thickness, InSe retains high mobility and direct band gap even for few-layers, which makes it a 2D material of huge interest for future electronics and opto-electronics. The electron mobilities of ~1000 $cm^2V^{-1}s^{-1}$ demonstrated at room temperature[1–3] in InSe devices are the highest values reported for an n-type 2D material so far. GaSe, on the other hand, is a p-type material with a band gap of 2.11 eV in bulk[14–16] and well known for its optical properties. In terms of electronic transport, few-layered GaSe has revealed mobilities of 0.1–0.6 $cm^2V^{-1}s^{-1}$ when integrated as a channel into field-effect transistors (FETs).[8–9] Unlike InSe, GaSe is not a high-mobility material due to the presence of heavy holes but it is still very appealing for opto-electronics,[8,17–18] single-photon emission,[19] non-linear optics[20] and terahertz applications[11]. Despite many promising properties of InSe and GaSe which could exceed those of TMDCs in various applications, limited work has been done exploiting their intrinsic properties due to their instability in ambience.

Though GaSe has been demonstrated to be highly air-sensitive degrading readily on interaction with air species,[17,21–22] the question whether InSe is air-sensitive or not has been a subject of intense debate within the scientific community. Some reports have claimed it to be relatively

stable with no observable degradation over time,[4,22–24] and extracted high mobilities under normal atmospheric conditions,[2–3] while others observed that it degrades in ambience on contact with water and oxygen.[25–27] Even standard process steps of device fabrication involving lithographic patterning, resist spinning and solvents' dips can cause considerable structural damage, degrading the quality of the material and resulting in poor performance of the devices.[7,28] It is worth mentioning that most previous reports which reported high mobility on bare InSe, used thicker layers (>30 nm) and shadow masks to fabricate their devices.[2–5] However, as InSe layer thickness approaches the quantum confinement limit, it becomes increasingly sensitive to environmental influences such as oxygen, moisture, charge traps in the dielectric and contaminations from chemical solvents, leading to fast and uncontrollable morphological changes and poor device performance. It is thus safe to say that InSe has better air-stability than GaSe, nevertheless thin layers of InSe tend to suffer from considerable degradation when exposed to air as compared to its bulk. Therefore, in order to achieve high performance and stable devices based on these materials, effective encapsulation techniques should be developed to protect InSe and GaSe layers against degradation and maintain their structural integrity.

Recently the techniques of dry oxidation[27] and seeded atomic layer deposition (ALD)[29] have been demonstrated to overcome the instability of InSe. While both techniques use oxide-based encapsulation, they provide only top encapsulation whereas the bottom surface of InSe rests on the SiO_2 substrate. SiO_2 has been demonstrated to be an unsuitable dielectric for 2D materials as it deteriorates the material's quality and device performance by inducing charge disorder at the interface due to scattering from charge traps, impurities and surface roughness.[30–31] InSe-based FETs have previously shown substantial hysteresis and unreliability in their I-V characteristics

due to charge trapping at the SiO_2/InSe interface and hydration on the SiO_2 surface.[2] Moreover, ALD encapsulation requires lithography to fabricate devices which as discussed earlier, leads to further unreliability of devices. For GaSe, hexagonal boron nitride (hBN) as a top encapsulation has been recently reported, with a focus on its optoelectronic properties.[17] Though ambient-stable GaSe photodetectors were achieved, the performance was inferior to those reported on SiO_2 substrate.[8,18,32]

Here we report a hBN-based encapsulation, where 2D layers of InSe and GaSe are sandwiched between two layers of hBN; top hBN passivating the 2D layer from the ambience and bottom hBN acting as a spacer and suppressing charge transfer to the 2D layer from SiO_2 substrate. To fabricate the devices from fully encapsulated InSe and GaSe layers, we employ the technique of lithography-free via-contacts,[33] which are metal contacts embedded within hBN flakes and allow to simultaneously achieve encapsulation and electrical connection to the underlying 2D layer without any direct lithographic patterning. Based on our results we find that full hBN encapsulation preserves InSe in its pristine form and suppresses its degradation with time under ambient conditions. Consequently, electronic properties of encapsulated InSe are significantly improved, leading to a two-terminal field-effect mobility (μ_{FE}) ranging 30–120 $cm^2V^{-1}s^{-1}$ and an on/off ratio of 10^4 at room temperature as compared to μ_{FE} of mere ~1 $cm^2V^{-1}s^{-1}$ obtained for unencapsulated devices. In addition, encapsulated InSe devices are stable for a prolonged period of time overcoming its limitation to be air-sensitive. On integrating full hBN encapsulation into few-layered GaSe, we improved photoluminescence (PL) dramatically and obtained a high photoresponsivity of 84.2 AW^{-1} at 405 nm. The full hBN encapsulation technique, therefore, allowed us to passivate the sensitive layers of InSe and GaSe from various degrading factors and probe their unaltered properties to achieve both high-performance and long-term ambient

stability. It is a robust technique and easily transferrable to other complex 2D materials which might not be compatible to the chemistry of ALD and dry oxidation techniques, thereby, opening ways towards investigation of 2D materials which were restricted in their fundamental study or applications so far due to environmental sensitivity.

EXPERIMENTAL SECTION:

The hBN/2D/hBN (here 2D: InSe, GaSe) heterostructures are fabricated by using the vdW transfer technique as described by L. Wang *et al.*.[34] In order to avoid exposing 2D layers to the ambience, the process steps from exfoliation of its bulk crystal until the 2D layers are fully covered between top and bottom hBN are performed inside a nitrogen-filled glovebox. Via-contacts used for the devices are fabricated as shown in the schematic of Figure 1a. hBN flakes (30-40 nm thick, crack and residue-free) exfoliated onto a SiO_2(285 nm)/Si substrate are identified using optical contrast, and subsequently etched into desired electrode patterns using reactive ion etching. The etched holes are then filled with 20 nm palladium (Pd)/40 nm gold (Au) metal by electron beam evaporation. The via-contact is then picked up and laminated onto the targeted 2D flake resting on a bottom hBN in a way that all via metal electrodes cover the flake (Figure 1b). After full encapsulation, the whole assembly is moved out of the glovebox for fabricating further metal extensions to the via-metal and contact pads where the probes can be placed to carry out the electrical measurements (see Methods and Supporting Information for details on the fabrication process). Figure 1b, c show the schematic and the optical micrograph of one such InSe–via device, where black solid lines (in the enlarged image of Figure 1c) show via-metal in an intimate contact with the underlying InSe layer. The heterostructures are fabricated in a contamination free environment, so that the layers have clean and impurity free interfaces. Multiple via-contacts in one hBN flake allow us to contact and measure multiple devices on one

single InSe flake. Figure 1d, e show the schematic and the optical image of an unencapsulated InSe device, respectively, fabricated by electron beam lithography and metal deposition on InSe layers exfoliated directly onto a SiO_2(285 nm)/Si substrate. For a consistent comparison, both encapsulated and unencapsulated devices are fabricated with the same thickness of InSe i.e. 9.6 nm or 12 layers (as confirmed with atomic force microscopy) and same contact metal configuration (Pd: 20 nm)/Au: 40 nm) deposited by electron beam evaporation.

RESULTS AND DISCUSSION:

To demonstrate the effect of full hBN encapsulation on the stability of InSe, we employed micro-PL measurements to adjacent surfaces of exposed and protected InSe. Figure 2a, b show the PL spectra obtained for both samples at 297 K and 4.2 K respectively. It is clearly evident that at both temperatures, hBN encapsulation significantly enhances the PL spectra by yielding narrower and sharper peaks as compared to the unencapsulated InSe due to crystalline and atomically flat layers of hBN. The slight red-shift in the peaks of hBN encapsulated sample is due to the different dielectric environment than SiO_2. The prominent effect of hBN encapsulation is seen at 4.2 K (Figure 2b), where the PL linewidth narrows down to give a full-width at half maximum (FWHM) of ~12 meV in contrast to 36–38 meV obtained for the exposed InSe of the same thickness. This significant reduction of the PL linewidth in the encapsulated sample indicates fabrication of a high-quality hBN/InSe/hBN vdW heterostructure and a defect-free dielectric environment provided for the InSe layer. At 297 K, the linewidth of both samples broadens and shows a red-shift (approx. 50 meV) as seen in Figure 2a due to interaction with acoustic and optical phonons.[35–36] Furthermore, the encapsulated InSe shows about 5 times higher PL intensity which further confirms the suppression of surface charge traps and defects by using bottom hBN substrate.[31,35] Our results thus comply with previous reports on TMDCs,

where hBN encapsulation preserves InSe from ambience and reduces the charge disorder by spatially separating the TMDC layer from the SiO_2 surface, giving rise to a significantly narrower PL linewidth.[35–38]

The same samples are measured over time to test their long-term stability under ambient conditions. Figure 2c, d reveal the PL spectra measured at room temperature under normal atmospheric conditions (see Methods for detailed PL specifications) for a time period of 8 weeks. Between consecutive measurements, both samples are stored in dark under ambient conditions, allowing the ambient exposure to affect both devices in the same manner. Figure 2e shows that the PL peak intensity of the encapsulated InSe is intact for almost 4 weeks after which it starts to decline gradually, whereas for the unencapsulated sample the PL intensity has almost vanished after 2 weeks. Balakrishnan *et al*.[23] have attributed the reduction in the PL intensity to the formation of In_2O_3 as InSe thin layers are exposed to air, higher temperatures and focused lasers. The trend in Figure 2 indicates that the stability of the InSe layers is greatly enhanced by using hBN encapsulation which preserves InSe from the complex physical and chemical changes occurring when it comes in contact with air.

To investigate the quality of hBN encapsulated InSe FETs, electrical performance of both encapsulated and unencapsulated devices is measured in back gate configuration. The transfer curves of both devices (Figure 3a) show an n-type FET behavior due to intrinsic doping of InSe layers as predicted previously.[2–4] The room temperature two-terminal field effect mobility (μ_{FE}) is extracted by using the following equation –

$$\mu_{FE} = \frac{dI_{DS}}{dV_G} \cdot \frac{L}{WC_iV_{DS}}$$

Where L and W are the length and width of the channel, I_{DS} and V_{DS} are source-drain current and voltage, V_G is the back gate voltage and C_i is the capacitance per unit area. C_i estimated for the encapsulated device is 0.108×10^{-7} F/cm^2 (full calculation in Supporting Information). For the 9.6 nm InSe–via encapsulated device shown in Figure 1c, the extracted μ_{FE} is 30 cm^{2}V^{-1}s^{-1} with an on/off ratio of 10^4. For other InSe–via devices with InSe thicknesses of 8–12 nm, mobility ranging 30–120 cm^{2}V^{-1}s^{-1} is obtained (Figure S2). In addition, hBN encapsulated device shows negligible hysteresis in comparison to the unencapsulated device as well as to previously reported devices using ALD and dry oxidation as encapsulation where substantial hysteresis was observed[27,29] due to trapped charge carriers at the InSe–SiO_2 interface.[2,31,39] Large hysteresis can give rise to further unreliability issues, *e.g*. extraction of field-effect mobility which in a hysteric curve becomes strongly dependent on the gate sweep direction.[40] For this particular unencapsulated device we extracted a mobility of ~0.47 cm^{2}V^{-1}s^{-1} (in forward sweep), which is the lower limit of the mobility due to large hysteresis (Figure S3). On testing multiple unencapsulated devices, we obtained large hysteresis in all devices, poor mobility values of ~1 cm^{2}V^{-1}s^{-1} and on/off ratios of few hundreds. The output curve of the encapsulated device (Figure 3b) reveals linear characteristics indicating formation of ohmic contacts between the Pd/Au metal used in the via-contact and the underlying 9.6 nm InSe layer. However, we could not produce ohmic and reliable contacts for unencapsulated InSe FETs as revealed in Figure 3c, which might be due to degradation of InSe prior to the metal deposition, leading to tunnel barriers at the metal–InSe interface[5]. The InSe channel area, in addition, is continuously degrading due to air exposure. Thus, as evident from our results, full hBN encapsulation is a reliable and effective passivation technique for InSe and yield a stable charge transport, greatly enhanced μ_{FE} and on/off ratio as compared to the unencapsulated devices.

To investigate the long-term stability of InSe devices, the samples were stored and measured in air for 15 days. The transfer curve of the encapsulated device (Figure 4a) shows very stable and consistent charge transport for over 2 weeks, whereas the unencapsulated device has large hysteresis and low on-currents (Figure 4b). The evolution of field effect mobility and on/off ratio with time for both devices is shown in Figure 4c and d, respectively. The unencapsulated device shows poorer mobility and lower on/off ratio than the encapsulated device from the beginning and continues to deteriorate further with time. (Note that the unencapsulated device was fabricated and measured within few hours from the time of exfoliation to minimize the degradation). The performance of the encapsulated device, on the other hand, stays intact throughout the measured time period. This indicates that InSe is susceptible to degradation in air but also to standard process steps of device fabrication. During the whole process, InSe layers come in contact with various pre- and post-lithographic solvents, which may induce structural damage, tunnel barriers and pinning of the Fermi level.[33] The presence of tunnel barriers and fermi level pinning results in non-ohmic contacts, lower on-current and mobility[29,41] as seen in Figure 3c for the unencapsulated devices. Wei *et al.*[26] have shown that adsorption of oxygen atoms into the InSe structure causes a serious hampering of the electronic properties with mobility and other FET parameters to decrease 2-3 orders in magnitude. Therefore, it is essential to passivate InSe from the ambience, and at the same time from other detrimental processes where its structural integrity can be compromised. In this regard, the top and bottom hBN encapsulation scheme is extremely useful as it prevents InSe from all sorts of degradation and disorder, and allows us to study its intrinsic properties.

Subsequently, we integrated the full hBN encapsulation technique into GaSe, another emerging 2D material belonging to the same family as InSe but far more sensitive under ambient

conditions. The effectiveness of hBN encapsulation in suppressing GaSe degradation is supported by low-temperature PL measurements (Figure 5a, b) which show a significant improvement in the spectra of the encapsulated GaSe as compared to the unencapsulated layer. On measuring various thicknesses of GaSe layers (18–28 nm), we observed 10 times higher PL peak intensity when it is encapsulated in top and bottom hBN, whereas unencapsulated GaSe shows significant PL reduction within 3 hours from the time of exfoliation. Since GaSe finds a majority of its applications in optics, the large band gap of hBN (~ 5.7 eV)[42] is highly advantageous, as it stays transparent for the wavelengths where GaSe is optically active. The photoresponse obtained for our GaSe–via device under global illumination of blue laser (405 nm) at various powers is shown in Figure 5c and d. As the device is illuminated by higher laser powers, I_{DS} increases proportionally due to increased number of electron-hole pairs generated. In response to a pulsed illumination of 405 nm, the device shows a fast photoswitching behavior and maintains long-term stability of its photoresponse (Figure 5c). The photocurrent ($I_{PH} = I_{light} - I_{dark}$) and responsivity ($R = I_{PH}/PA$; P is incident power density, A is exposed device area) measured at V_G = -80 V and V_{DS} = 2 V show a linear dependence on incident power densities as seen in Figure 5d. At an incident power density of 0.3 mW/cm^2, we achieved a responsivity of 84.2 AW^{-1}, which is a major improvement over top encapsulated GaSe photodetectors reported previously[17].

CONCLUSIONS:

The sensitivity of few-layered InSe and GaSe towards ambience, bottom dielectrics and lithography processes makes the assessment of their intrinsic properties difficult. We demonstrate that in order to study their pristine properties, their full encapsulation in hBN layers is extremely advantageous as it prevents the 2D layers from ambient degradation as well as from

the charge disorder at the SiO_2 surface, leading to the fabrication of high quality and stable vdW heterostructures. The fully encapsulated InSe and GaSe devices show greatly enhanced and ambient stable performance as compared to their unencapsulated counterparts. hBN due to its inertness, atomically flat surface and absence of charge traps is, therefore, an optimal encapsulation for fabricating reliable InSe and GaSe-based devices and studying their pristine properties. In future, it can be applied to other sensitive 2D materials which might then supersede existing materials in terms of properties and performance.

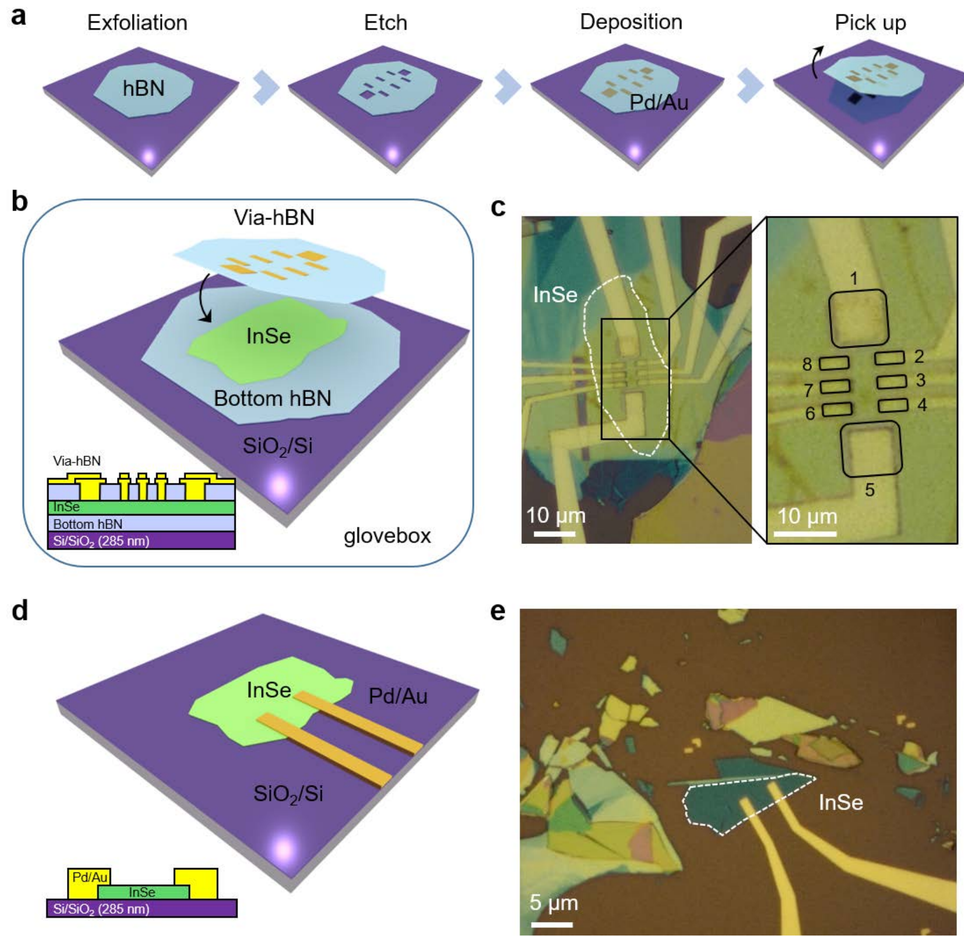

Figure 1. Fabrication of Pd/Au via-contacts and two configurations of InSe-based device geometries investigated in this work. (a) Step-wise illustration of the via-contact fabrication process. (b) Schematic of the InSe–via device when via-contact hBN covers InSe in a glovebox to encapsulate it and to form electrical connection. (c) Optical image of the InSe–via device measured in this work. InSe flake 9.6 nm thick (white dashed line) is sandwiched between bottom hBN and top via-hBN. The black solid lines in the enlarged image highlight the Pd/Au metal contacts embedded in hBN and forming van der Waals contact with the underlying InSe layer. (d), (e) Schematic and optical image of an unencapsulated device (9.6 nm InSe) on SiO_2 substrate and metal electrodes fabricated by depositing Pd/Au metal. White dashed line indicates the InSe flake.

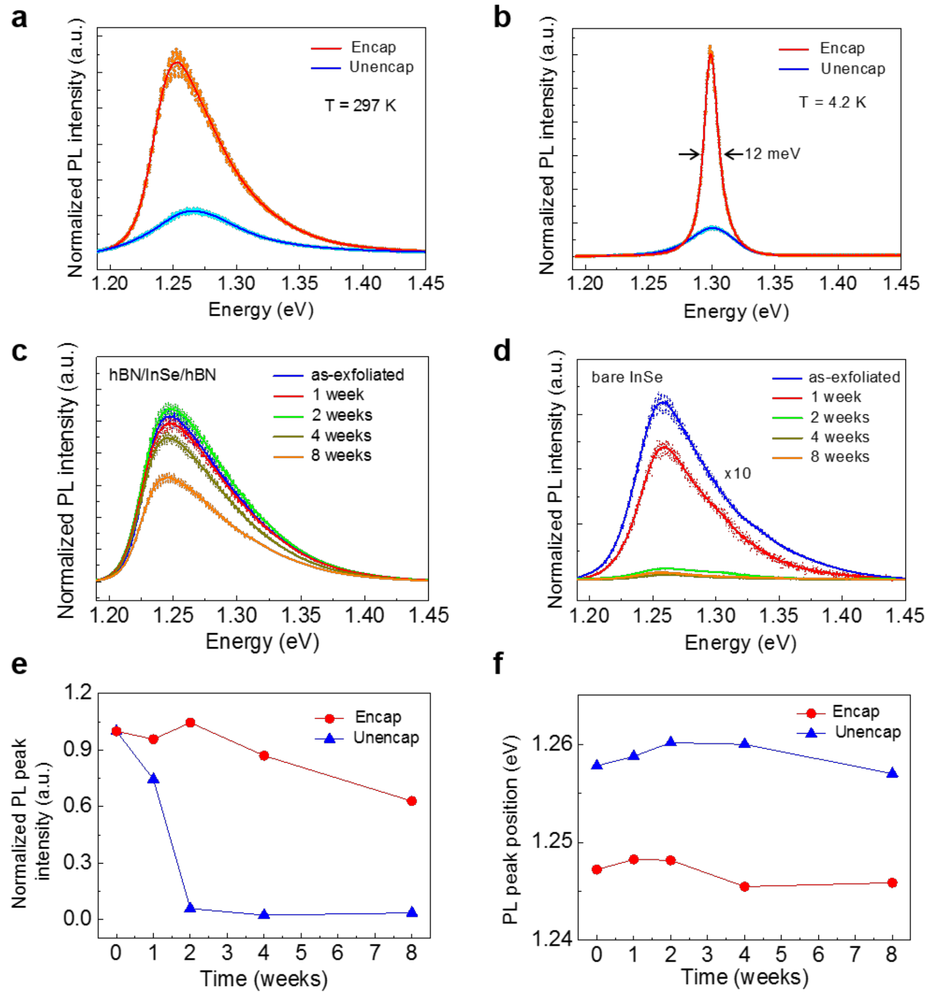

Figure 2. Photoluminescence (PL) spectra measured for encapsulated and unencapsulated InSe, demonstrating high quality and ambient stability of fully hBN encapsulated InSe. PL spectra measured for both samples (a) at 297 K, showing higher intensity and red-shifted PL peak for encapsulated InSe and (b) at 4.2 K, showing a narrower linewidth with FWHM of 12 meV for encapsulated InSe. (c), (d) Evolution of the PL spectra with time for both encapsulated and unencapsulated InSe at room temperature, respectively, stored under ambient conditions. (e), (f) Normalized PL peak intensity and PL peak position measured with time, showing structural instability of InSe when exposed to the ambience, whereas the encapsulated sample stays intact over 4 weeks.

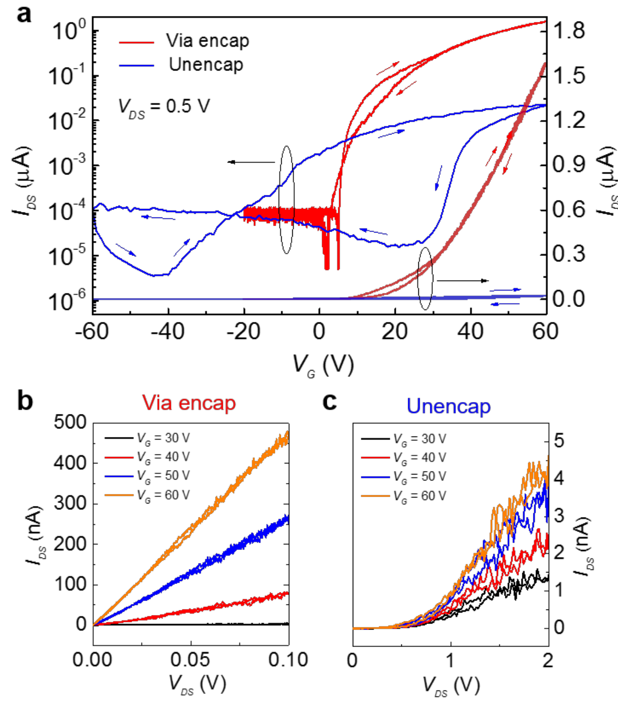

Figure 3. Electrical characterization of encapsulated InSe–via device and unencapsulated InSe device shown in Figure 1c, d respectively. (a) Transfer characteristics (linear and semi-log) of both devices at V_{DS} = 0.5 V measured in back gate configuration. The small arrows show the direction of the gate sweep. (b) Output characteristics of InSe–via encapsulated device for back gate voltages from +30 V to +60 V with steps of 10 V, showing linear characteristics indicating ohmic behavior. (c) Output characteristics of unencapsulated InSe device measured at back gate voltages from +30 V to +60 V with steps of 10 V, showing non-linear behavior. Note that current level in the unencapsulated device is significantly lower than the encapsulated device even in large V_{DS} regimes.

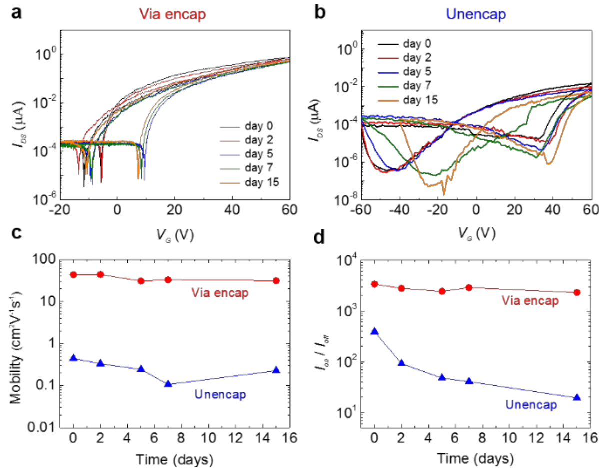

Figure 4. Transfer characteristics and FET parameters measured with time to investigate the stability of via-encapsulated and unencapsulated InSe devices. (a) Semi-log transfer curve of via-encapsulated device at V_{DS} = 0.5 V measured over 15 days. The on- and off-currents are highly reproducible with time indicating an ambient stable device. (b) Semi-log transfer curve of the unencapsulated device measured under same conditions as the encapsulated device. Huge hysteresis and unstable current demonstrates unreliable device characteristics. Evolution of (c) mobility and (d) on/off ratio, with time for both device configurations. Both parameters are intact for encapsulated device, while unencapsulated device degrades at a fast pace.

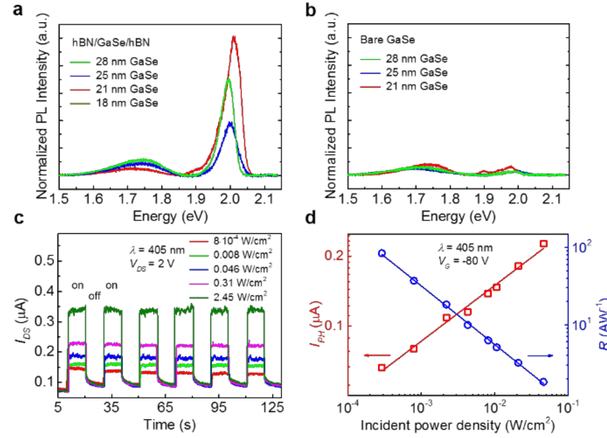

Figure 5. Optical characterization of fully encapsulated GaSe devices. (a), (b) Photoluminescence spectra at 4.2 K measured for fully encapsulated GaSe layers of various thicknesses, showing intense PL peaks at ~2.0 eV and unencapsulated GaSe showing PL reduction due to fast degradation under ambience, respectively. (c) Photoswitching response obtained for a pulsed illumination of 405 nm at V_G = -80 V, V_{DS} = 2 V and various laser power densities. (d) Photocurrent (red open squares) and responsivity (blue open dots) as a function of incident power density at V_G = -80 V and V_{DS} = 2 V. Red and blue straight lines are obtained by fitting the measured data and show a linear dependence on laser power.

METHODS:

Bulk crystals of InSe and GaSe (2H phase with a purity of 99.995%) are bought commercially from *2dSemiconductors* and *hqgraphene*, respectively. The crystals are mechanically exfoliated by Scotch tape (model BT-130E-SL bought from *TELTEC GmBH*) inside a nitrogen-filled glovebox and stacked between top and bottom hBN using "van der Waals transfer" technique, described in detail in Supporting Information. To fabricate via-contacts, holes are etched into hBN flakes using reactive ion etching (Oxford RIE) with a gas mixture of SF_6 and O_2. The holes are deposited with (Pd: 20 nm)/Au: 40 nm) using an e-beam evaporator. For lift-off process, the samples are dipped into acetone for at least 2 hours followed by rinsing in isopropanol and nitrogen blow dry. The extended metal leads to the hBN/InSe/via-hBN stack are fabricated using e-beam lithography under a poly(methyl methacrylate) (PMMA) e-beam resist mask followed by metal deposition (Cr: 2 nm/Pd: 20 nm/Au: 40 nm) and standard lift-off process as described above. Low-temperature micro-PL measurements are carried out using a LHe cryostat system. The excitation pump was a cw frequency-doubled Nd:YAG laser at a wavelength of 532 nm. The power was 10 µW focused on a spot diameter of 3 µm. The spectra are captured on a liquid nitrogen cooled silicon CCD deep-depletion camera after being dispersed in a 300 lines/mm grating spectrometer. Electrical measurements are performed using a parameter analyzer (Agilent, 4155C) and photoresponse using Lake Shore probe station (Model CPX-VF) equipped with a cw-blue laser diode at 405 nm wavelength. All electrical and photocurrent measurements are carried out in air and at room temperature.

ASSOCIATED CONTENT

Supporting Information Available: Details on vdW heterostructure fabrication. Electrical characterization of other InSe–via devices. This material is available free of charge via the Internet at http://pubs.acs.org.

AUTHOR INFORMATION

Corresponding Author

*James Hone (email: jh2228@columbia.edu)

*Artur Erbe (email: a.erbe@hzdr.de)

Author Contributions

H.A. exfoliated InSe and GaSe from bulk crystals and fabricated vdW heterostructures of hBN and InSe or GaSe. Y.J. fabricated via-contacts and prepared devices by electron-beam lithography. T.V., H.S. and H.A. performed PL measurements. H.A. measured charge transport and photoresponse in the devices. K.W and T.T. provided hBN crystals. All authors discussed the results and participated in the preparation of the manuscript. J.C.H. and A.E. supervised the project.

Notes

The authors declare no competing financial interest.

ACKNOWLEDGMENTS

We thank D. Rhodes, N. R. Finney and G. Arefe for their help in device fabrication and subject matter discussion and F. Kilibarda for drawing the schematics. Growth of hexagonal boron nitride crystals was supported by the Elemental Strategy Initiative conducted by the MEXT, Japan, A3 Foresight by JSPS and the CREST (JPMJCR15F3), JST. This work was kindly

supported by the Initiative and Networking Fund of the Helmholtz Association of German Research Centers through the International Helmholtz Research School for Nanoelectronic Networks, IHRS NANONET (VH-KO-606) and INSPIRE grant from Center of Advancing Electronics Dresden (cfaed).

REFERENCES

(1) Bandurin, D. A.; Tyurnina, A. V.; Yu, G. L.; Mishchenko, A.; Zólyomi, V.; Morozov, S. V.; Kumar, R. K.; Gorbachev, R. V.; Kudrynskyi, Z. R.; Pezzini, S.; *et al.* High Electron Mobility, Quantum Hall Effect and Anomalous Optical Response in Atomically Thin InSe. *Nat. Nanotechnol.* **2017**, *12* , 223–227.

(2) Sucharitakul, S.; Goble, N. J.; Kumar, U. R.; Sankar, R.; Bogorad, Z. A.; Chou, F.-C.; Chen, Y.-T.; Gao, X. P. A. Intrinsic Electron Mobility Exceeding 1000 cm^2/(Vs) in Multilayer InSe FETs. *Nano Lett.* **2015**, *15*, 3815–3819.

(3) Feng, W.; Zheng, W.; Cao, W.; Hu, P. Back Gated Multilayer InSe Transistors with Enhanced Carrier Mobilities *Via* the Suppression of Carrier Scattering from a Dielectric Interface. *Adv. Mater.* **2014**, *26*, 6587–6593.

(4) Feng, W.; Zhou, X.; Tian, W. Q.; Zheng, W.; Hu, P. Performance Improvement of Multilayer InSe Transistors with Optimized Metal Contacts. *Phys. Chem. Chem. Phys.* **2015**, *17*, 3653–3658.

(5) Yang, H. W.; Hsieh, H. F.; Chen, R. S.; Ho, C. H.; Lee, K. Y.; Chao, L. C. Ultraefficient Ultraviolet and Visible Light Sensing and Ohmic Contacts in High-Mobility InSe Nanoflake Photodetectors Fabricated by the Focused Ion Beam Technique. *ACS Appl. Mater. Interfaces* **2018**, *10*, 5740–5749.

(6) Ho, C.-H.; Lin, M.-H.; Chuang, C.-A.; Yeh, B.-X.; Chu, Y.-J. 2D Multilayer Inse - An

Applicable 1000 nm Light Emitter and Absorber. *Imaging Appl. Opt.* **2016**, JT3A.5.

(7) Tamalampudi, S. R.; Lu, Y.-Y.; Kumar, U. R.; Sankar, R.; Liao, C.-D.; Moorthy, B. K.; Cheng, C.-H.; Chou, F. C.; Chen, Y.-T. High Performance and Bendable Few-Layered InSe Photodetectors with Broad Spectral Response. *Nano Lett.* **2014**, *14*, 2800–2806.

(8) Abderrahmane, A.; Jung, P.-G.; Kim, N.-H.; Ko, P. J.; Sandhu, A. Gate-Tunable Optoelectronic Properties of a Nano-Layered GaSe Photodetector. *Opt. Mater. Express* **2017**, *7*, 587–592.

(9) Late, D. J.; Liu, B.; Luo, J.; Yan, A.; Matte, H. S. S. R.; Grayson, M.; Rao, C. N. R.; Dravid, V. P. GaS and GaSe Ultrathin Layer Transistors. *Adv. Mater.* **2012**, *24*, 3549–3554.

(10) Savchyn, V. P.; Kytsai, V. B. Photoelectric Properties of Heterostructures Based on Thermo-Oxidated GaSe and InSe Crystals. *Thin Solid Films* **2000**, *361*, 123–125.

(11) Shi, W.; Ding, Y. J. A Monochromatic and High-Power Terahertz Source Tunable in the Ranges of 2.7–38.4 and 58.2–3540 μm for Variety of Potential Applications. *Appl. Phys. Lett.* **2004**, *84*, 1635–1637.

(12) Kuroda, N.; Nishina, Y. Resonance Raman Scattering Study on Exciton and Polaron Anisotropies in InSe. *Solid State Commun.* **1980**, *34*, 481–484.

(13) Mudd, G. W.; Svatek, S. A.; Ren, T.; Patanè, A.; Makarovsky, O.; Eaves, L.; Beton, P. H.; Kovalyuk, Z. D.; Lashkarev, G. V.; Kudrynskyi, Z. R.; *et al.* Tuning the Bandgap of Exfoliated InSe Nanosheets by Quantum Confinement. *Adv. Mater.* **2013**, *25*, 5714–5718.

(14) Le Toullec, R.; Balkanski, M.; Besson, J. M.; Kuhn, A. Optical Absorption Edge of a New GaSe Polytype. *Phys. Lett. A* **1975**, *55*, 245–246.

(15) Bube, R. H.; Lind, E. L. Photoconductivity of Gallium Selenide Crystals. *Phys. Rev.* **1959**,

115, 1159–1164.

(16) Minder, R.; Ottaviani, G.; Canali, C. Charge Transport in Layer Semiconductors. *J. Phys. Chem. Solids* **1976**, *37*, 417–424.

(17) Zhao, Q.; Frisenda, R.; Gant, P.; Perez de Lara, D.; Munuera, C.; Garcia-Hernandez, M.; Niu, Y.; Wang, T.; Jie, W.; Castellanos-Gomez, A. Toward Air Stability of Thin GaSe Devices: Avoiding Environmental and Laser-Induced Degradation by Encapsulation. *Adv. Funct. Mater.* **2018**, *28*.

(18) Hu, P.; Wen, Z.; Wang, L.; Tan, P.; Xiao, K. Synthesis of Few-Layer GaSe Nanosheets for High Performance Photodetectors. *ACS Nano* **2012**, *6*, 5988–5994.

(19) Tonndorf, P.; Schwarz, S.; Kern, J.; Niehues, I.; Del Pozo-Zamudio, O.; Dmitriev, A. I.; Bakhtinov, A. P.; Borisenko, D. N.; Kolesnikov, N. N.; Tartakovskii, A. I.; *et al.* Single-Photon Emitters in GaSe. *2D Mater.* **2017**, *4*.

(20) Jie, W.; Chen, X.; Li, D.; Xie, L.; Hui, Y. Y.; Lau, S. P.; Cui, X.; Hao, J. Layer-Dependent Nonlinear Optical Properties and Stability of Non-Centrosymmetric Modification in Few-Layer GaSe Sheets. *Angew. Chemie - Int. Ed.* **2015**, *54*, 1185–1189.

(21) Rahaman, M.; Rodriguez, R. D.; Monecke, M.; Lopez-Rivera, S. A.; Zahn, D. R. T. GaSe Oxidation in Air: from Bulk to Monolayers. *Semicond. Sci. Technol.* **2017**, *32*.

(22) Del Pozo-Zamudio, O.; Schwarz, S.; Klein, J.; Schofield, R. C.; Chekhovich, E. A.; Ceylan, O.; Margapoti, E.; Dmitriev, A. I.; Lashkarev, G. V.; Borisenko, D. N.; *et al.* Photoluminescence and Raman Investigation of Stability of InSe and GaSe Thin Films. **2015**, arXiv: 1506.05619 [cond-mat. mes-hall].

(23) Balakrishnan, N.; Kudrynskyi, Z. R.; Smith, E. F.; Fay, M. W.; Makarovsky, O.; Kovalyuk, Z. D.; Eaves, L.; Beton, P. H.; Patanè, A. Engineering P–N Junctions and

Bandgap Tuning of InSe Nanolayers by Controlled Oxidation. *2D Mater.* **2017**, *4*.

(24) Politano, A.; Chiarello, G.; Samnakay, R.; Liu, G.; Gürbulak, B.; Duman, S.; Balandin, A. A.; Boukhvalov, D. W. The Influence of Chemical Reactivity of Surface Defects on Ambient-Stable InSe-Based Nanodevices. *Nanoscale* **2016**, *8*, 8474–8479.

(25) Shi, L.; Zhou, Q.; Zhao, Y.; Ouyang, Y.; Ling, C.; Li, Q.; Wang, J. Oxidation Mechanism and Protection Strategy of Ultrathin Indium Selenide: Insight from Theory. *J. Phys. Chem. Lett.* **2017**, *8*, 4368–4373.

(26) Wei, X.; Dong, C.; Xu, A.; Li, X.; Macdonald, D. D. Oxygen-Induced Degradation of the Electronic Properties of Thin-Layer InSe. *Phys. Chem. Chem. Phys.* **2018**, *20*, 2238–2250.

(27) Ho, P.-H.; Chang, Y.-R.; Chu, Y.-C.; Li, M.-K.; Tsai, C.-A.; Wang, W.-H.; Ho, C.-H.; Chen, C.-W.; Chiu, P.-W. High-Mobility InSe Transistors: the Role of Surface Oxides. *ACS Nano* **2017**, *11*, 7362–7370.

(28) Arora, H.; Schönherr, T.; Erbe, A. Electrical characterization of two-dimensional materials and their heterostructures. *IOP Conf. Ser. Mater. Sci. Eng.* **2017**, *198*, 012002.

(29) Wells, S. A.; Henning, A.; Gish, J. T.; Sangwan, V. K.; Lauhon, L. J.; Hersam, M. C. Supressing Ambient Degradation of Exfoliated InSe Nanosheet Devices Via Seeded Atomic Layer Deposition Encapsulation. *Nano Lett.* **2018**, *18*, 7876–7882.

(30) Dean, C. R.; Young, A. F.; Meric, I.; Lee, C.; Wang, L.; Sorgenfrei, S.; Watanabe, K.; Taniguchi, T.; Kim, P.; Shepard, K. L.; *et al.* Boron Nitride Substrates for High-Quality Graphene Electronics. *Nat. Nanotechnol.* **2010**, *5*, 722–726.

(31) Lee, G.-H.; Cui, X.; Kim, Y. D.; Arefe, G.; Zhang, X.; Lee, C.-H.; Ye, F.; Watanabe, K.; Taniguchi, T.; Kim, P.; *et al.* Highly Stable, Dual-Gated MoS_2 Transistors Encapsulated by Hexagonal Boron Nitride with Gate-Controllable Contact, Resistance, and Threshold

Voltage. *ACS Nano* **2015**, *9*, 7019–7026.

(32) Cao, Y.; Cai, K.; Hu, P.; Zhao, L.; Yan, T.; Luo, W.; Zhang, X.; Wu, X.; Wang, K.; Zheng, H. Strong Enhancement of Photoresponsivity with Shrinking the Electrodes Spacing in Few Layer GaSe Photodetectors. *Sci. Rep.* **2015**, *5*.

(33) Telford, E. J.; Benyamini, A.; Rhodes, D.; Wang, D.; Jung, Y.; Zangiabadi, A.; Watanabe, K.; Taniguchi, T.; Jia, S.; Barmak, K.; *et al.* Via Method for Lithography Free Contact and Preservation of 2D Materials. *Nano Lett.* **2018**, *18*, 1416–1420.

(34) Wang, L.; Meric, I.; Huang, P. Y.; Gao, Q.; Gao, Y.; Tran, H.; Taniguchi, T.;Watanabe, K.; Campos, L. M.; Muller, D. A.; *et al.* One-Dimensional Electrical Contact to a Two-Dimensional Material. *Science.* **2013**, *342*, 614–617.

(35) Cadiz, F.; Courtade, E.; Robert, C.; Wang, G.; Shen, Y.; Cai, H.; Taniguchi, T.; Watanabe, K.; Carrere, H.; Lagarde, D.; *et al.* Excitonic Linewidth Approaching the Homogeneous Limit in MoS_2-Based Van Der Waals Heterostructures. *Phys. Rev. X* **2017**, *7*.

(36) Manca, M.; Glazov, M. M.; Robert, C.; Cadiz, F.; Taniguchi, T.; Watanabe, K.; Courtade, E.; Amand, T.; Renucci, P.; Marie, X.; *et al.* Enabling Valley Selective Exciton Scattering in Monolayer WSe_2 Through Upconversion. *Nat. Commun.* **2017**, *8*, 1–7.

(37) Cadiz, F.; Robert, C.; Wang, G.; Kong, W.; Fan, X.; Blei, M.; Lagarde, D.; Gay, M.; Manca, M.; Taniguchi, T.; *et al.* Ultra-Low Power Threshold for Laser Induced Changes in Optical Properties of 2D Molybdenum Dichalcogenides. *2D Mater.* ***2016**, 3.*

(38) Obafunso, A. A.; Ardelean, V. J.; Shepard, D. G.; Wang, J.; Antony, A.; Taniguchi, T.; Watanabe, K.;, Heinz, T. F.; Strauf, S.; Zhu, X.-Y.; *et al.* Approaching the Intrinsic Photoluminescence Linewidth in Transition Metal Dichalcogenide Monolayers. *2D Mater.*

2017, *4*.

(39) Doganov, R. A.; O’Farrell, E. C. T.; Koenig, S. P.; Yeo, Y.; Ziletti, A.; Carvalho, A.; Campbell, D. K.; Coker, D. F.; Watanabe, K.; Taniguchi, T.; *et al.* Transport Properties of Pristine Few-Layer Black Phosphorus by Van Der Waals Passivation in an Inert Atmosphere. *Nat. Commun.* **2015**, *6*.

(40) Egginger, M.; Bauer, S.; Schwödiauer, R.; Neugebauer, H.; Sariciftci, N. S. Current Versus Gate Voltage Hysteresis in Organic Field Effect Transistors. *Monatshefte fur Chemie* **2009**, *140*, 735–750.

(41) Xiao, K. J.; Carvalho, A.; Castro Neto, A. H. Defects and Oxidation Resilience in InSe. *Phys. Rev. B* **2017**, *96*.

(42) Watanabe, K.; Taniguchi, T.; Kanda, H. Direct-Bandgap Properties and Evidence for Ultraviolet Lasing of Hexagonal Boron Nitride Single Crystal. *Nat. Mater.* **2004**, *3*, 404–409.

For Table of Contents Only